06

Modeling of shock-wave loading of magnesium silicates on the example of forsterite

© K.K. Maevskii[1,2]

[1]Lavrentyev Institute of Hydrodynamics, Siberian Branch, Russian Academy of Sciences,
630090 Novosibirsk, Russia
[2]Novosibirsk State University,
630090 Novosibirsk, Russia
e-mail: konstantinm@hydro.nsc.ru

Received April 1, 2022
Revised September 15, 2022
Accepted September 25, 2022

The results of modeling the shock-wave loading of Mg_2SiO_4 forsterite, which in this case is considered as a mixture of SiO_2 quartz and MgO periclase, are presented. The model is based on the assumption that the components of the mixture under shock-wave loading are in thermodynamic equilibrium. The model allows us to reliably describe the phase transition region. The components of the investigated material are considered as a mixture of low and high pressure phases. Polymorphic phase transitions of quartz and periclase are taken into account in the calculation of forsterite in pressure range from 1 to 1000 GPa. The results are verified by experimental data obtained in dynamic experiments.

Keywords: Equation of state, shock adiabat, thermodynamic equality, magnesium silicates, forsterite.

DOI: 10.21883/0000000000

Introduction

Interest in studies of the high-energy effect on magnesium silicates and, in particular, on forsterite Mg_2SiO_4 is due to the fact that these materials prevail in the Earth's mantle. Magnesium silicates and their high pressure phases are major components of the Earth and possibly of other inner planets of the Earth group. In this regard, forsterite, for which there are experimental data on high-energy effects, can be used in simulation of planetary collisions, which are an important process in the formation and evolution of planets [1]. A detailed understanding of both the physical and chemical processes that occur during and just after the collision of astronomical bodies motivates an accurate description of forsterite at pressures and temperatures significantly exceeding those corresponding to the interior of the Earth [2]. Besides, the discovery of new exoplanets around other stars in our galaxy raises new questions about the diversity of planetary architecture, and how such planets might form and evolve [3–5]. There is a growing interest in experimental studies of geological materials under conditions of ultrahigh pressure and temperature to solve both new and old problems in the science of the Earth and planets [6,7]. Knowledge of the composition and mineralogy of planets helps to determine their evolution and internal structure [8]. The forsterite parameters under shock-wave loading were experimentally studied in the range of 200 to 950 GPa and supplemented by theoretical calculations [2]. Studies of enstatite $Mg_2[Si_2O_6]$ and forsterite using shock-wave compression are summarized in [9,10].

High-energy effect leads to phase transformations of many materials. Experimental studies of phase diagrams at high pressures, phase transitions in magnesium oxide — quartz $MgO-SiO_2$ systems were carried out in [11]. In [12] it is noted that forsterite has several phase transitions at pressures below 200 GPa. The authors [13] obtained shock adiabats showing several slope changes in the pressure range between 270 and 470 GPa, which were interpreted as corresponding to regions of phase transformations. On the contrary, no signs of a phase transition above 200 GPa along the shock adiabat were observed in [11], this directly contradicts the results in [13]. Data on wave and mass velocities in these experiments show a linear growth and no signs of any phase transformations. With such results, further study of the shock adiabat of forsterite is necessary for better understanding of this material properties and making its equation of state in ranges of the pressure and temperature, which are important for simulating inner planets and planetary collision processes [2]. It was also shown in [12] that at pressures corresponding to the lower mantle of the Earth, there is no stable compound with the composition Mg_2SiO_4. So, reaching the equilibrium state from initially homogeneous forsterite crystal requires decomposition into at least two compounds.

The phase diagram under shock compression up to 200 GPa of Mg_2SiO_4 was investigated [9]. Note that the key question relates to the Mg_2SiO_4 dissociation along the shock adiabat, and for this reason it would be important to confirm the presence of MgO or $MgSiO_3$ in shock-wave studies of Mg_2SiO_4. Earlier in [14] it was noted that the Mg_2SiO_4 dissociation into oxides MgO and SiO_2 (stishovite) was observed. These experiments were carried out at a pressure of 33 GPa, which corresponds to the pressure in the Earth's mantle at a depth of 1000 km. The same

question is discussed in papers [11,15], where it is noted that the description of behavior, in particular for $MgSiO_3$ and Mg_2SiO_4, is still far from satisfactory one, especially at high pressures above 2 Mbar. It was supposed in [16] that a mixed phase mode exists for single crystal forsterite subjected to pressures of 50 to 120 GPa, and that this mode exists in a smaller pressure range for polycrystalline forsterite. It is assumed that the transformation into a high pressure mixture of $MgO + MgSiO_3$ of perovskite is completed at 100 GPa for initial material. i. e. forsterite [9]. In paper [17] at normal temperature, the structure of forsterite under compression to 48 GPa was observed. At 50 GPa a phase transition to a new structure (forsterite II) occurs, and then transition to forsterite III at 58 GPa. In this case, a total volume decreasing by $\sim 10\%$ is observed. The discussion about the occurrence of phase transitions along shock adiabats is currently ongoing. Note that the experimental study of the pressure effect on the kinetics of phase transformations is even more difficult problem than the study of phase equilibria under pressure. This explains the very small number of studies in this direction [18].

1. Problem formulation

Based on the availability of data on the dissociation of magnesium silicates into components, it was suggested that these components are MgO and SiO_2. Many papers, in particular [19], were associated with the study of these oxides in connection with the study of the composition of the Earth's mantle. In this case, phase transitions of silicates can be considered as phase transitions of the components into which they decompose at appropriate pressures. Simulation requires a model of shock-wave loading of materials with components experiencing a phase transition under high dynamic loads. A reliable description for materials undergoing phase transition was obtained using the thermodynamic equilibrium model [20]. Based on this model, calculations of shock-wave loading of forsterite, considered as a mixture of quartz SiO_2 and periclase MgO in the ratio 1 : 2, are performed, based on the stoichiometric ratio. It is assumed that the components of the material under study under shock-wave loading are in thermodynamic equilibrium (equality of velocities, pressures and temperatures). For a two-phase medium this assumption was previously applied, in particular, in [21]. The model under study makes it possible to reliably describe the results of shock-wave experiments in the pressure range of 1 GPa to 10 TPa for both solid and porous samples of pure materials, including SiO_2 and MgO. Complementing the system of equations of dynamic compatibility with the condition of equality of temperatures of the mixture components, dependences are written that can be interpreted as shock adiabats of heterogeneous sample [22–24]. At the same time, considering the material under study in the phase transition region as a mixture of low pressure and high pressure phases, it is possible to reliably describe the region of polymorphic phase transition for various substances, including oxides [25,26].

2. Calculation procedure

The Mie-Gruneisen equation of state is used to simulate the behavior of condensed phases:

$$P(\rho, T) = P_c(\rho) + P_T(T), \qquad P_T(\rho, T) = \Gamma\rho E_T(T), \tag{1}$$

where

$$E_T(T) = c_V(T - T_0), \tag{2}$$

P_C, is the potential component of pressure, P_T, is the thermal component; E_T is the thermal component of pressure of specific energy, c_V is the thermal capacity, and T_0 is the initial temperature. The perfect gas equation is taken for gas. The conditions for dynamic compatibility at the wave front are written out in the form of the Rankine–Hugoniot relationships, which express the conditions for the conservation of mass, pulse, and energy [27]:

$$\frac{\rho}{\rho_0} = \frac{D}{D-U}, \quad P = \rho_0 UD, \quad E = \frac{1}{2}P\left(\frac{1}{\rho_0} - \frac{1}{\rho}\right), \tag{3}$$

where ρ, ρ_0 are current and initial density of the condensed component, U, D are mass and wave velocities. Taking into account the area of this model application, for pressure values over 1 GPa, the values of energy and pressure under normal conditions are not considered. The conditions for conservation of pulse and energy flows are given for the mixture as a whole. In this case, for the mass flow, the conservation conditions are written out for each component separately. This approach makes it possible to calculate not only the compression of the material as a whole, but also to determine the compression of each component separately. For the material containing n solid components with initial volume fractions μ_{n0}, the following expressions are obtained:

$$P = \frac{\sum\limits_{i=1}^{n} A_i \frac{\mu_{i0}}{\sigma_i}\left[\left(h_i - \frac{k_i+1}{k_i-1}\right)\sigma_i^{k_i} + \frac{2k_1\sigma_i}{k_i-1} - h_i - 1\right]}{\sum\limits_{i=1}^{n}\frac{\mu_{i0}}{\sigma_i}h_i + \left(\frac{h_g}{\sigma_g}\right)\left(1 - \sum\limits_{i=1}^{n}\mu_{i0}\right) - 1}, \tag{4}$$

$$h_i = \frac{2}{\Gamma_i} + 1, \qquad h_g = \frac{2}{\gamma - 1} + 1.$$

Here $\sigma_i = \rho_i/\rho_{i0}$, $\sigma_g = \rho_g/\rho_{g0}$ are compression ratios of the corresponding component $i = 1 \ldots n$, and ρ_g, ρ_{g0} are current and initial gas densities with adiabatic exponent, $\gamma = 1.41$. The function $\Gamma = P_T V/E_T$ determines the contribution of the thermal components, while it explicitly depends only on the temperature [28]. Complementing (4) with the condition of equality of the component temperatures and with the equations of state of each component, the dependencies are found that can be considered as shock adiabats of the heterogeneous material $P(U)$ or $D(U)$ (A, k are coefficients in the equations of state).

Thermodynamic parameters of heterogeneous materials (values of pressure, density, temperature) are calculated in the region of polymorphic phase transition, based on the assumption that the material under study is a mixture of the low pressure phase and the high pressure phase [24–26]. When simulating in the phase transition region, it is assumed that the volume fraction of the low-pressure α-phase passed into the high-pressure phase. According to the experimental data the pressure value corresponding to the beginning of the phase transition process is determined. The value of the fraction α is close to linear one depending on the internal energy increment: $\alpha = \Delta E/kf$, while $kf = E_f - E_b$, $\Delta E = E - E_b$ (E — current internal energy, E_b — internal energy at the beginning of the phase transition, E_f — internal energy at the end of the phase transition when all the material passed into the high pressure phase). kf parameter makes it possible to describe the experimental data for the samples under study with different porosity values. When calculating the shock adiabat, three sections of simulation are specified for materials experiencing polymorphic phase transition [24]:

$$\begin{cases} E \le E_b, & \alpha = 0, \\ E_g \le E \le_f, & \alpha = \Delta E/kf, \\ E \le E_f, & \alpha = 1. \end{cases} \qquad (5)$$

The following values are determined for SiO_2 and MgO: the parameter kf is equal to 2.5 and 15.0 kJ/g, the pressure of the phase transition beginning is 11 and 250 GPa, respectively.

3. Simulation results

The simulation results of the thermodynamic parameters and the data obtained on the basis of experiments are shown in Fig. 1 for amorphous quartz with a density $\rho_0 = 2.204\,\text{g/cm}^3$, taking into account the phase transition in pressure–compression coordinates. Before the phase transition beginning at a pressure of 11 GPa, the calculation coincides with the shock adiabat of quartz (low pressure phase). At pressures above 40 GPa we assume that the phase transition completed; the calculation corresponds to the shock adiabat of stishovite considered as a high-pressure phase of quartz with the same initial density as the original sample. In this case, the porosity m (the ratio of the monolithic sample density to the porous sample density) for stishovite will be 1.63.

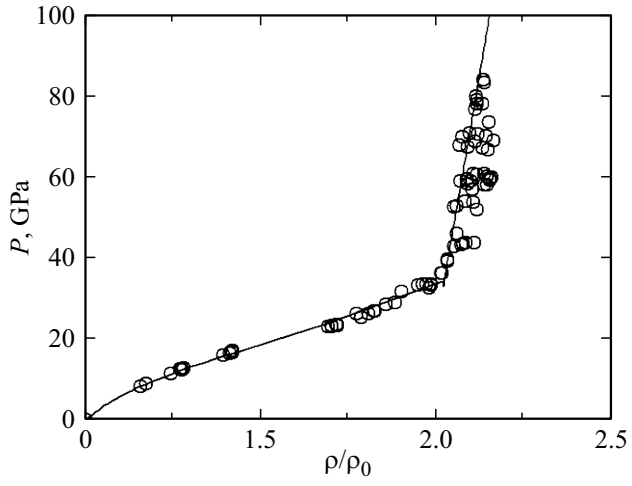

Figure 1. Shock adiabat of quartz. Data [29,30].

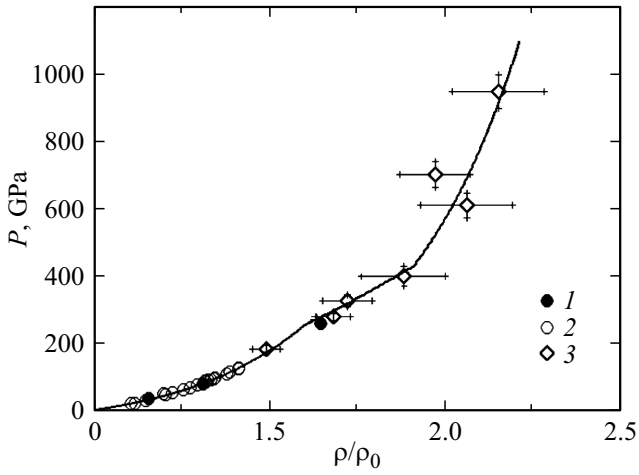

Figure 2. Shock adiabat of MgO. Calculation — solid line. Data *1* — [31], *2* — [32] and *3* — [33].

For MgO the simulation results and experimental data are shown in Fig. 2 in pressure–compression variables. The model parameters that were used in the calculations for SiO_2 and MgO oxides are shown in the Table for the low (1) and high pressure (2) phases, respectively.

The ability to describe the behavior of pure materials made it possible to calculate, among other things, the behavior of mixtures, which, in particular, include quartz. Fig. 3 shows the calculation in variables pressure–compression of a mixture of aluminum and quartz at ratio of volume fractions 50 : 50, 40 : 60, 30 : 70, and for comparison the shock adiabat for pure quartz is given, using experimental data from [30,34,35]. As noted by the authors of paper [34], the additive model for such mixture description did not allow the shock adiabat of quartz restoration. This is due to the fact that the additivity rule in this approach is approximate, since it assumes the actually non-existent correspondence of compression of components in heterogeneous mixtures and the shock compression of homogeneous components [36,37]. A reliable description of the results of shock-wave loading of quartz with other materials is given in [38]. Mixtures of quartz with paraffin, tungsten of various compositions, as well as with Teflon and epoxy resin were simulated in the compression range up to 80 GPa.

Using this method for calculating heterogeneous materials, the experimental results of shock-wave loading of various nitrides experiencing a phase transition under dynamic loads [25], as well as of their mixtures, are reliably

SiO_2 and MgO parameters for low pressure phases — 1 and high pressure phases — 2

Parameter	MgO (1)	MgO (2)	SiO_2 (1)	SiO_2 (2)
A, GPa	39.62	40.0	14.5	130
ρ, g/cm^3	3.584	4.050	2.204	4.310
n	4	3.99	4.05	3.00
c_v, J/(kg·K)	937.2	937.2	1100	1100
$\Gamma(T_0)$	1.05	1.07	1.3	1.3
$\Gamma(T^*)$	0.90	1.06	0.80	0.09
T, K·10^3	23	23	20	20
$\Gamma(T_\infty)$	0.500	0.500	0.500	0.500

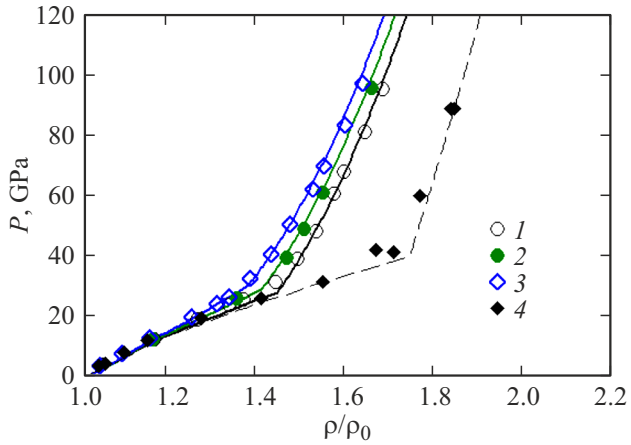

Figure 3. Shock adiabats of mixtures of aluminum with quartz and of quartz. The solid curves are the shock adiabats of mixtures, the dashed line is the adiabat of quartz. Experiment: mixtures of Al and SiO_2 having a ratio of mole fractions: *1* — 50 : 50, *2* — 40 : 60, *3* — 30 : 70 [34]; *4* — quartz [35].

described. The possibility of simulating the parameters of a mixture with two components experiencing phase transition under shock-wave loading was shown.

Taking into account the observed dissociation of Mg_2SiO_4 into oxides MgO and SiO_2 in the form of stishovite [14] at pressures of 33 GPa, it can be assumed that forsterite at this pressure value will also contain stishovite. The model calculation showed that at this pressure value most of the SiO_2 actually passed into the high-pressure phase, i. e. stishovite.

Based on the assumption of possible dissociation of magnesium silicates under pressure, calculations were made for forsterite as a mixture of oxides SiO_2 and MgO. Simulation results for forsterite $\rho_0 = 3.273$ g/cm^3 are shown in Fig. 4 in variables pressure–mass velocity, porosity value $m = 1.03$, 1.08 was determined by the average value of the studied samples. The data of two groups of experiments for samples with an average density of 3.01 and 2.95 g/cm^3 are also shown here. The deviation, in particular, is explained by the scattering of density values. A description of the behavior of porous samples within the accuracy of the experiment is obtained.

The simulation results for forsterite in the pressure range up to 1 TPa and the data [13] are shown in Fig. 5, 6 taking into account the phase transitions of SiO_2 and MgO. For MgO the phase transition region is determined in the range 250–400 GPa.

It is of interest to compare the simulation results for mixtures with the same composition, which presumably arises during the forsterite dissociation into two oxides. Model calculations for porous mixtures of periclase and quartz in the molar ratio $MgO(67)SiO_2(33)$, having density values $\rho_0 = 1.894$ and 1.693 g/cm^3 are shown in Fig. 7, 8; the porosity value for them is $m = 1.675$ and 1.84, respectively. Here are the data obtained on the basis of experiments [28].

A reliable description of the available experimental data was obtained, while the parameters determined for oxides were used to describe mixtures with these oxides, as well as for forsterite, considering it as a mixture of oxides at the level of experimental accuracy.

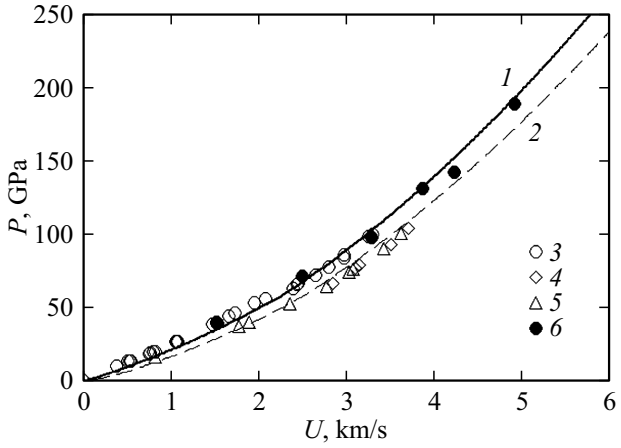

Figure 4. Shock adiabat of forsterite $\rho_0 = 3.273$ g/cm^3. Calculation — curve *1* — $m = 1.03$, *2* — $m = 1.08$; data *3, 5* — [29], *4* — [32], *6* — [39].

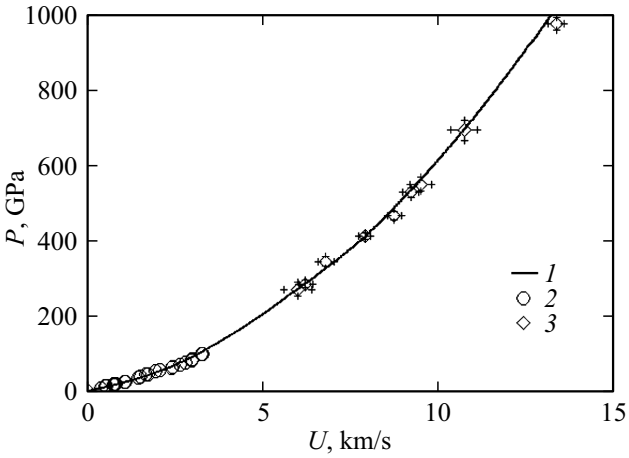

Figure 5. Shock adiabat of forsterite in variables pressure–mass velocity $\rho_0 = 3.273$ g/cm^3. Calculation — curve *1*; data *2* — [29], *3* — [13].

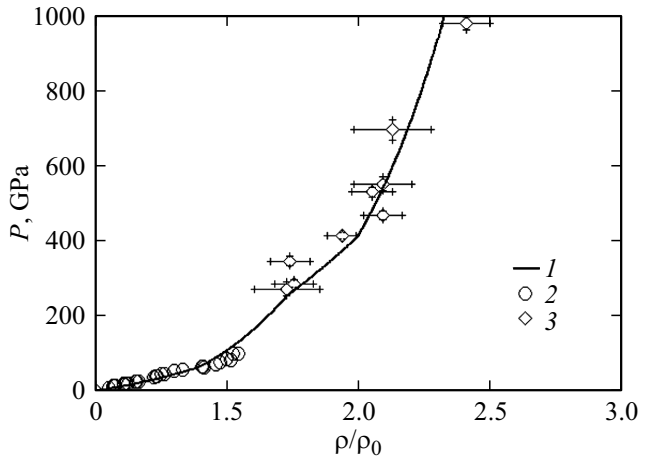

Figure 6. Shock adiabat of forsterite in variables pressure–compression $\rho_0 = 3.273\,\mathrm{g/cm^3}$. Calculation — curve *1*; data *2* — [29], *3* — [13].

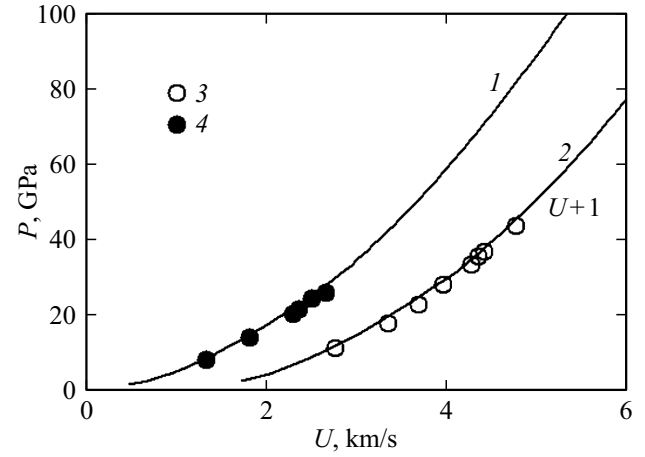

Figure 7. Shock adiabat of mixture of periclase and quartz in variables pressure–mass velocity. *1* — $\rho_0 = 1.894\,\mathrm{g/cm^3}$, *2* — $\rho_0 = 1.693\,\mathrm{g/cm^3}$. ($m$ 1.675; 1.84) [29,30].

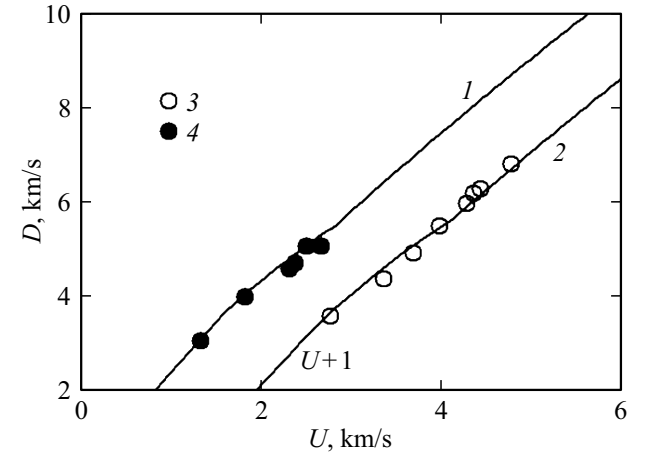

Figure 8. Shock adiabat of mixture of periclase and quartz in variables wave–mass velocity. Designations as in Fig. 7.

4. Results and discussion

The simulation results show that calculations by the thermodynamically equilibrium model, based on the assumption of the forsterite Mg_2SiO_4 dissociation into SiO_2 and MgO, in according to the stoichiometric ratio reliably describe the available data obtained on the basis of experiments. Considering the components of the material under study in the phase transition region as a mixture of the low pressure and high pressure phases, the model used makes it possible to reliably describe several phase transitions. In this case, it becomes possible to take into account the high-pressure phase transition for MgO.

Taking into account the reliable description of experimental data for forsterite up to 1000 GPa, which exceeds the pressure value in the center of the Earth by three times [40], it can be assumed that this approach will be useful in calculations for more massive planets. This approach can be used for other magnesium silicates as well. The joint results for various silicates will make it possible to predict pressure and temperature profiles depending on their composition, and will also allow us to estimate the contribution of phase transitions of materials to the density change of the Earth's mantle.

The good agreement between the model calculations and the results obtained for forsterite based on experiments suggests that the procedure used will allow us to reliably describe the behavior of other similar materials containing components that experience the phase transition under dynamic action.

Funding

This study was supported by the Budget Project III.22.3.1.

Conflict of interest

The authors declare that they have no conflict of interest.

References

[1] E.J. Davies, M.S. Duncan, S. Root, R.G. Kraus, D.K. Spaulding, S.B. Jacobsen, S.T. Stewart. JGR Planets, **126**, e2020JE006745 (2021). DOI: 10.1029/2020JE006745
[2] S. Root, J.P. Townsend, E. Davies, R.W. Lemke, D.E. Bliss, D.E. Fratanduono, R.G. Kraus, M. Millot, D.K. Spaulding, L. Shulenburger1, S.T. Stewart, S.B. Jacobsen. Geophys. Res. Lett., **45**, 3865 (2018). DOI: 10.1029/2017GL076931
[3] T.S. Duffy, R.F. Smith. Front. Earth Sci., **7**, 23 (2019). DOI: 10.3389/feart.2019.00023
[4] H. Niu, A.R. Oganov, A., X.Q. Chen, D. Li. Sci. Rep., **5**, 18347 (2016). DOI: 10.1038/srep18347
[5] K. Umemoto, R.M. Wentzcovitch, S. Wu, M. Ji, C.Z. Wang, K.M. Ho. Earth. Planet. Sci. Lett., **478**, 40 (2017). DOI: 10.1016/j.epsl.2017.08.032
[6] W.J. Borucki. Rep. Prog. Phys., **79**, 036901 (2016). DOI: 10.1088/0034-4885/79/3/036901

[7] P.E. Driscoll. Planetary Interiors, Magnetic Fields, and Habitability. In: Handbook of Exoplanets. Ed. by H. Deeg, J. Belmonte (Springer, Cham., 2018), DOI: 10.1007/978-3-319-55333-7_76
[8] C.T. Unterborn, J.E. Kabbes, J.S. Pigott, D.M. Reaman, W.R. Panero. Astrophys. J., **793**, 2 (2014). DOI: 10.1088/0004-637X/793/2/124
[9] J.L. Mosenfelder, P.D. Asimow, T.J.J. Geophys. Res., **112**, B06208 (2007). DOI: 10.1029/2006JB004364
[10] J.L. Mosenfelder, P.D. Asimow, D.J. Frost, D.C. Rubie, T.J. Ahrens. J. Geophys. Res., **114**, B01203 (2009). DOI: 10.1029/2008JB005900
[11] R.M. Bolis, G. Morard, T. Vinci, A. Ravasio, E. Bambrink, M. Guarguaglini, M. Koenig, R. Musella, F. Remus, J. Bouchet, N. Ozaki, K. Miyanishi, T. Sekine, Y. Sakawa, T. Sano, R. Kodama, F. Guyot, A. Benuzzi-Mounaix. Geophys. Res. Lett., **43**, 9475 (2016). DOI: 10.1002/2016GL070466
[12] M.G. Newman, R.G. Kraus, M.C. Akin, J.V. Bernier, A.M. Dillman, M.A. Homel, S. Lee, J. Lind, J.L. Mosenfelder, D.C. Pagan, N.W. Sinclair, P.D. Asimow. Geophys. Res. Lett., **45**, 8129 (2018). DOI: 10.1029/2018GL077996
[13] T. Sekine, N. Ozaki, K. Miyanishi, Y. Asaumi, T. Kimura, B. Albertazzi, Y. Sato, Y. Sakawa, T. Sano, S. Sugita, T. Matsui, R. Kodama. Sci. Adv., **2**, e1600157 (2016). DOI: 10.1126/sciadv.1600157
[14] M. Kumazawa, H. Sawamoto, E. Ohtani, K. Mazaki. Nature, **247**, 356 (1974).
[15] D.K. Spaulding, R.S. McWilliams, R. Jeanloz, J.H. Eggert, P.M. Celliers, D.G. Hicks, G.W. Collins, R.F. Smith. Phys. Rev. Lett., **108**, 065701 (2012). DOI: 10.1103/PhysRevLett.108.065701
[16] Y. Syono, T. Goto, J. Sato, H. Takei. J. Geophys. Res., **86**, 6181 (1981). DOI: 10.1029/JB086iB07p06181
[17] G.J. Finkelstein, P.K. Dera, S. Jahn, A.R. Oganov, C.M. Holl, Y. Meng, T.S. Duffy. Am. Mineral., **99** (1), 35 (2014). DOI: 10.2138/am.2014.4526
[18] X.G. Huang, X.H. Yuan, Z.A. Chen, F.S. Liu, W.M. Bai. Sci. China Earth. Sci., **592016**, 619 (2016). DOI: 10.1007/s11430-015-5231-2
[19] L.V. Altshuler, R.F. Trunin, G.V. Simakov. Izv. AN SSSR. Ser. Fizika Zemli, **29**, 10 (1) (in Russian).
[20] K.K. Maevskii, S.A. Kinelovskii. Tech. Phys., **64**, 1090 (2019). DOI: 10.1134/S1063784219080127
[21] V.V. Milyavskii, V.E. Fortov, A.A. Frolova, K.V. Khishchenko, A.A. Charakhch'yan, L.V. Shurshalov. Comput. Math. Math. Phys., **46**, 873 (2006). DOI: 10.1134/S0965542506050113
[22] K.K. Maevskii K.K. AIP Conf. Proc., **2051**, 020181 (2018). DOI: 10.1063/1.5083424
[23] K.K. Maevskii. Tech. Phys., **66** (5), 791 (2021). DOI: 10.1134/S1063784221050145
[24] Maevskii K. AIP Conf. Proc., 2103, 020009 (2019). 10.1063/1.5099873
[25] K.K. Maevskii, S.A. Kinelovskii. High Temperature, **56** (6) 853 (2018). DOI: 10.1134/S0018151X18060172
[26] K.K. Maevskii. J. Phys. Conf. Series., **894**, 012057 (2017). DOI: 10.1088/1742-6596/894/1/012057
[27] Ya.B. Zel'dovich, Yu.P. Raizer, *Fizika udarnykh voln i vysokotemperaturnykh gidrodinamicheskikh yavlenii* (Fizmatlit, M., 2008), s. 519 (in Russian).
[28] K.K. Maevsky. ZhTF, **92** (1), 100 (2022) (in Russian). DOI: 10.21883/JTF.2022.01.51858.200-21
[29] S.P. Marsh (ed.) *LASL Shock Hugoniot Data* (Univ. California Press., Berkeley, 1980)
[30] P.R. Levashov, K.V. Khishchenko, I.V. Lomonosov, V.E. Fortov. AIP Conf. Proc., **706**, 87 (2004). http://www.ihed.ras.ru/rusbank/
[31] L.V. Altshuler, R.F. Trunin, G.V. Simakov. Izv. AN SSSR. Ser. Fizika Zemli, **29**, 10 (1) (in Russian).
[32] *Compendium of shock wave data*, ed. by M. Thiel (Livermore, Lawrence Livermore Laboratory, Report UCRL-50108, 1977), p. 401.
[33] K. Miyanishi, Y. Tange, N. Ozaki, T. Kimura, T. Sano, Y. Sakawa, T. Tsuchiya, R. Kodama. Phys. Rev. E, 92, 023103 (2015). DOI: 10.1103/PhysRevE.92.023103
[34] M.A. Podurets, G.V. Simakov, R.F. Trunin. Izv. AN SSSR **4**, 28 (1968) (in Russian).
[35] R.F. Trunin, G.V. Simakov, M.A. Podurets. Izv. AN SSSR **2**, 33 (1971) (in Russian).
[36] R.F. Trunin, *Issledovaniya ekstremal'nykh sostoyanii kondensirovannykh veshchestv metodom udarnykh voln. Uravneniya Gyugonio* (RFYaF−VNIIEF, Sarov, 2006), s. 137 (in Russian).
[37] A.A. Bakanova, I.P. Dudoladov, Yu.N. Sutulov. Prikladnaya mekhanika i tekh. fizika **6**, 167 (1972) (in Russian).
[38] K.K. Maevskii, S.A. Kinelovskii. AIP Conf. Proc., **1683**, 020132 (2015). 10.1063/1.4932822
[39] J.L. Mosenfelder, P.D. Asimow, T.J. Ahrens. J. Geophys. Res., *112*, B06208 (2007). DOI: 10.1029/2006JB004364
[40] A.M. Dziewonski, D.L. Anderson. Phys. Earth Planet. Inter., **25**, 297 (1981). DOI:10.1016/0031-9201(81)90046-7